A LEO Nano-Satellite Mission for the Detection of Lightning VHF Sferics

Ghulam Jaffer[1,2], Hans U. Eichelberger[2],
Konrad Schwingenschuh[2] and Otto Koudelka[1]
[1]Institute of Communication Networks and Satellite Communications
Graz University of Technology, Graz
[2]Space Research Institute, Austrian Academy of Sciences, Graz
Austria

1. Introduction

The LiNSAT is a proposed project for the detection of electromagnetic signatures produced by lightning strokes (Sferics) in very high frequency (VHF) range in low-earth-orbit (LEO) around 800 km. The satellite is 20 cm cube and weighs ~ 5 kg. The main scientific objective of the planned LiNSAT is the investigation of impulsive electromagnetic signals generated by electrical discharges in terrestrial thunderstorms (lightning), blizzards, volcanic eruptions, earthquakes and dust devils. These electromagnetic phenomena called Sferics cover the frequency range from a few Hertz (Schumann resonances) up to several GHz. Depending on the source mechanism, the wave power peaks at different frequencies, e.g. terrestrial lightning has a maximum power in the VLF and HF range, also trans-ionospheric pulses reaching at LEO and possibly to satellites in geostationary-Earth-orbit (GEO) peak at VHF. The global terrestrial lightning rate is in the order of 100 lightning flashes per second with an average energy per flash of about 10^9 Joule (Rakov and Uman 2003). Only a small percentage of the total energy is converted to electromagnetic radiation. Other forms are acoustic (thunder), optical and thermal, so the whole power of lightning flash is distributed into many chunks of energies. The signal strength received by a satellite radio experiment depends on the distance and the energy of a lightning stroke as well as on the orientation of the discharge channel.

The nano-satellite project under study emphasizes on the investigation of the global distribution and temporal variation of lightning phenomena using electromagnetic signals. In contrast to optical satellite observations the Sferics produced by lightning can be observed on the day and night side but with a smaller spatial resolution. We know from the Fast On-orbit Recording of Transient Events (FORTE) satellite mission (Jacobson, Knox et al. 1999) that at an altitude of about 1000 km the impulsive events produced by lightning can reach amplitudes up to 1 mV/m in a 1 MHz band around 40 MHz.

The LiNSAT is based on the design and the bus similar to the Austrian first astronomical nano-satellite TUGSat-1/ BRITE-Austria (Koudelka, Egger et al. 2009) which is scheduled to launch in April 2011. The LiNSAT will carry a broadband radio-frequency receiver payload for the investigation of Sferics. Special emphasis is on the investigation of transient

electromagnetic waves in the frequency range of 20 – 40 MHz, well above plasma frequency to avoid ionospheric attenuations. The on-board RF lightning triggering system is a special capability of the LiNSAT. The lightning experiment will also observe signals of ionospheric and magnetospheric origin. To avoid false signals detection (false alarm), pre-selectors on-board LiNSAT are part of the Sferics detector. Adaptive filters will be developed to differentiate terrestrial electromagnetic impulsive signals from ionospheric or magnetospheric signals.

One of the major challenges of using a nano-satellite for such a scientific payload is to integrate the lightning experiment antenna, receiver and data acquisition unit into the small nano-satellite structure. The optimization in this mission is to use one of the lightning antennas integrated into gravity gradient boom (GGB) that increases the sensitivity and directional capability of the satellite toward nadir direction. The section 5.1 and section 5.4 describe the space segment and modes of operation. Electromagnetic compatibility (EMC) issues are specially treated. Results of the payload in a simulated environment are presented in section 9.

The lightning emissions are the transient electrical activity of thunderstorms (primarily RS and IC activity) generates broadband electromagnetic radiations with spectrum range from ULF to UHF and also visible-light. A typical RS radiation peaks at ~10 kHz and an IC stroke produces radiations peaking at a slightly higher frequency at 40 kHz with 2 orders of magnitude less energy than a typical RS (Volland 1995). Electromagnetic radiations at these frequencies propagate through the earth - ionosphere waveguide, so can be observed at large distances, thousands of km from the source.

The lightning electromagnetic pulse (LEMP) is time-varying electromagnetic field that varies rapidly around 10 ns, reaches it maxima and then on its descending way is less fast around a few tens of μs and goes to a negligible value. The LEMP is very dangerous due to its ability to damage unprotected electronic devices. LEMPs are powerful radio emissions that radiate across a broad spectrum of frequencies from tens of kHz or lower to at least several hundred MHz as indicated by the inverse of LEMP rise time. As mentioned earlier, these broadband emissions reach LEO and possibly GEO, so the payload on-board LiNSAT will be designed as a broadband receiver.

The LiNSAT will operate in the VHF portion of the electromagnetic spectrum because lower frequency radio emissions (HF and below) often cannot penetrate through the earth's ionosphere and thus, do not reach LEO. Also, Sferics in higher band from VHF are less powerful, so, more difficult to detect. It complicates its detection and time tagging in the case of broadband VHF signals from LEO by the dispersive and refractive effects of the ionosphere. These effects become increasingly severe at lower frequencies in proportion to wavelength squared.

The LiNSAT radio receiver will record waveforms using a fixed-rate 200 MS/s, 12-bit digitizer that takes its input from either of a 3-antennas wideband sub-resonant monopole and a VHF receiver. The instrument utilizes a coarse trigger based on preset amplitude level to detect transient events.

As the radio emissions from natural lightning produce broadband transients in the VHF spectrum, so a potential source of false alarms for space based detection of other phenomena in the same band. One of the main objectives of the LiNSAT payload development on-board LEO nano-satellite is the need to characterize the Earth's radio background. The characterization is necessary for both transient signals, like those produced by lightning and continuous wave (CW) signals emitted by commercial broadcasting radio and television

stations. Even if a receiver is well-matched to the detection of broadband transients, CW signals can still degrade its sensitivity when many, powerful carriers exist within its bandwidth. Extensive experiments have been performed by the detection of natural and artificial lightning discharges in urban environment to visualize and verify the detectability of transient signals by LiNSAT payload in carrier-dominated radio environments and are discussed by (Jaffer and Schwingenschuh 2006a; Jaffer 2006b; Jaffer, Koudelka et al. 2008; Jaffer, Eichelberger et al. 2010d; Jaffer, Koudelka et al. 2010e; Jaffer 2011c; Jaffer and Koudelka 2011d)

2. Space heritage

2.1 CASSINI-HUYGENS

The LiNSAT research team in Graz is experienced in conducting field and particle experiments for planetary and interplanetary missions (Schwingenschuh, Molina-Cuberos et al. 2001). A milestone was the participation in an electric field experiment aboard ESA's HUYGENS mission, which for the first time explored the atmosphere of the Saturnian moon Titan (Fulchignoni, Ferri et al. 2005)**.** After a 7 years cruise to the Saturnian system and two close Titan encounters NASA's CASSINI orbiter released the HUYGENS probe on 25 December 2004. On 14 January 2005 the atmosphere of Titan was first detected by the HUYGENS Atmospheric Structure Instrument (HASI) accelerometers at an altitude of about 1500 km. About 5 minutes later at an altitude of 155 km the main parachute was deployed and the probe started to transmit data of the fully operational payload. About 2.5 h later the probe landed near the equator of Titan and continued to collect data for about one hour.

The orbit of the HUYGENS probe has been reconstructed using the data of the entry phase and of the descent under the parachute. The electric field sensor of HASI carried out measurements during the descent (2 hours and 27 minutes) and on the surface (32 minutes) about 3200 spectra in two frequency ranges from DC - 100 Hz and from DC - 11 kHz. The major emphasis of the data analysis is on the detection of electric and acoustic phenomena related to lightning (Fulchignoni, Ferri et al. 2005; Schwingenschuh, Hofe et al. 2006a; Schwingenschuh, Hofe et al. 2006b; Schwingenschuh, Besser et al. 2007; Schwingenschuh, Lichtenegger et al. 2008b; Schwingenschuh, Tokano et al. 2010).

Three methods are used to identify lightning in the atmosphere of Titan:

- Measurements of the low frequency electric field fluctuations produced by lightning strokes
- Detection of resonance frequencies on the Titan surface - ionosphere cavity
- Determination of the DC fair weather field of the global circuitry driven by lightning

Several impulsive events have been detected by the HASI lightning channel. The events were found to be similar to terrestrial Sferics and are most likely produced by lightning. Large convective clouds have been observed near the South Pole during the summer season and lightning generated low frequency electromagnetic waves can easily propagate by ionospheric reflection to the equatorial region. The existence of lightning would also be consistent with the detection of signals in the Schumann range and a very small fair weather field, but there is yet no confirmation by the CASSINI orbiter.

Contrary to the HUYGENS VLF lightning detector, the LiNSAT radio receiver is planned to operate in the VHF range which is less affected by the terrestrial ionosphere.

2.2 TUGSat-1/ BRITE

The predecessor of LiNSAT is the first Austrian nano-satellite TUGSat-1/BRITE-Austria, being developed by the Graz University of Technology with University of Vienna, Vienna University of Technology and the Space Flight Laboratory of University of Toronto (Canada) as partners. The scientific objective is the investigation of the brightness variation of massive luminous stars of magnitude +3.5. The satellite has a size of 20 x 20 x 20 cm with a mass of about 6 kg and carries a differential photometer as the science instrument. It will fly in a sun-synchronous orbit.

Figure 1 shows a mock-up of the TUGSat-1/ BRITRE nano-satellite. Power is generated by multiple body-mounted strings of triple- junction solar cells. The available power is about 6 W on average. Energy is stored in a 5.3 Ah Lithium-Ion battery. The power subsystem has been designed for direct energy transfer.
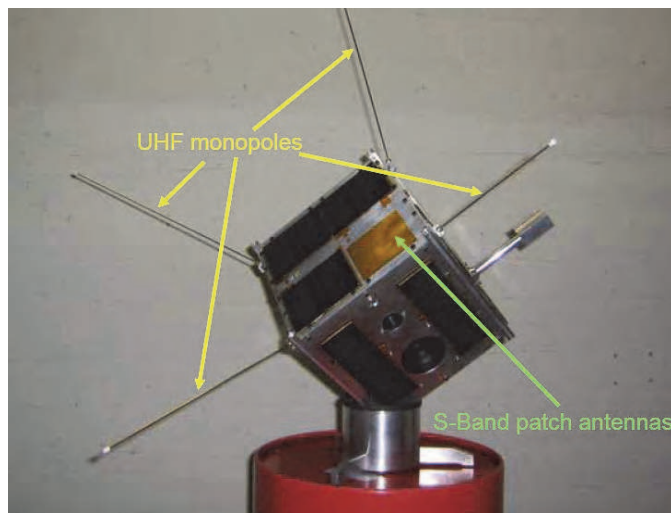

Fig. 1. TUGSat1 ADCS and antennas configuration.

A novelty is an advanced attitude determination and control system (ADCS) with three very small momentum wheels and a Star Tracker providing a pointing accuracy at the arc-minute level. Three on-board computers are installed in the spacecraft, one for housekeeping and telemetry, one for the science instrument and one for the ADCS.

The telemetry system comprises an S-band transmitter of about 0.5 W. It is capable for transmitting data with a minimum rate of 32 kbit/s. Data rates of up to 512 kbit/s are feasible with existing ground stations. The uplink is in the 70 cm band. A beacon in the 2 m band is also implemented (Koudelka, Egger et al. 2009).

Other objectives of TUGSat1 and LiNSAT are training of students, hands-on experience in conducting of a challenging space project and synergies between several scientific fields. The investigation of massive luminous stars with a precise star camera opens up new dimension for astronomers as observation of stars without interference by earth atmosphere can be carried out in LEO with such a small and low-cost spacecraft. Moreover, LiNSAT is a pure student satellite and will contribute as a low-cost atmospheric research platform.

3. Lightning discharges and classification

Lightning is a hazard, and sometimes a killer, as observed with severe storms and lightning strikes. Worldwide thousands of individual lightning discharges, including dramatic bolts, occur each day. The map in Figure 2 shows the geographic distribution of the frequency of strikes averaged over 8 years (1995 - 2003) of data collecting by NASA's Optical Transient Detector (OTD) and by the Lightning Imaging Sensor (LIS) on Tropical Rainfall Measurement (TRMM) (NASA 2011b). As indicated by the figure, the central part of Africa has been an area with the most lightning strikes; almost all of South America is prone to frequent electrical storm activity. A different perspective by looking at the distribution of lightning strikes worldwide average lightning strikes per square km per year can be seen in the same figure.
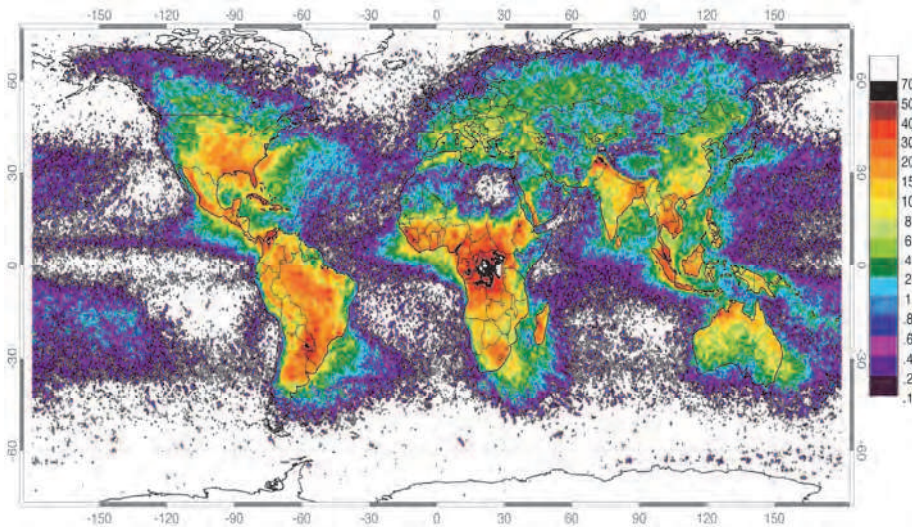
Fig. 2. Global distribution of lightning April 1995 – February 2003 from the combined observation of the NASA OTD (4/95-3/0) and LIS (1/98-2/03) instruments. Courtesy NASA TRMM team (NASA 2011a).

Each lightning strike exhibit unique signature and streak lightning being the most-commonly observed in the world. That is actually a return stroke (RS) that is the visible part of the lightning stroke. The majority of strokes occur within a cloud or clouds (IC), as indicated by Figure 3. Fair weather field is ~ 150 V/m close to the surface of earth. this field changes significantly the cloud electric field underneath (~ 10 kV/m) and within (~ 100 kV/m) the cloud (Uman 2001).

4. Lightning detection

It is well known from the very beginning of radio technology that lightning is a source of interference in amplitude-modulated (AM) radio reception. In fact before the radio use in transmissions/ broadcasting had shown that lightning causes distinctive noise in a radio channel, so that in this sense lightning detection can be said to pre-date other uses of the radio. Radio measurements of lightning were made extensively until the 1960's, although
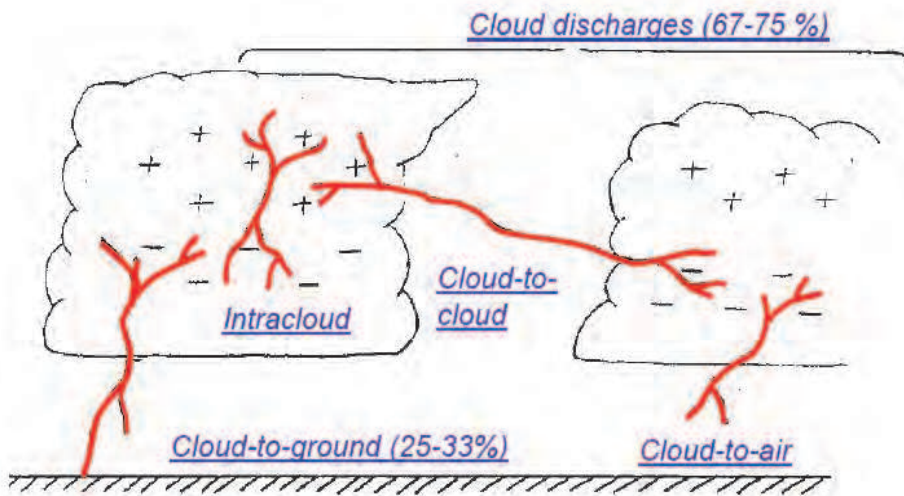
Fig. 3. The lightning classification indicates that almost two third of the lightning discharges occur within and inter- cloud that has direct impact on air traffic. Adapted from (Rakov and Uman 2003).

mainly with the purpose of improving radio transmissions. Some differences between optical and RF detection are elaborated in Figure 4.
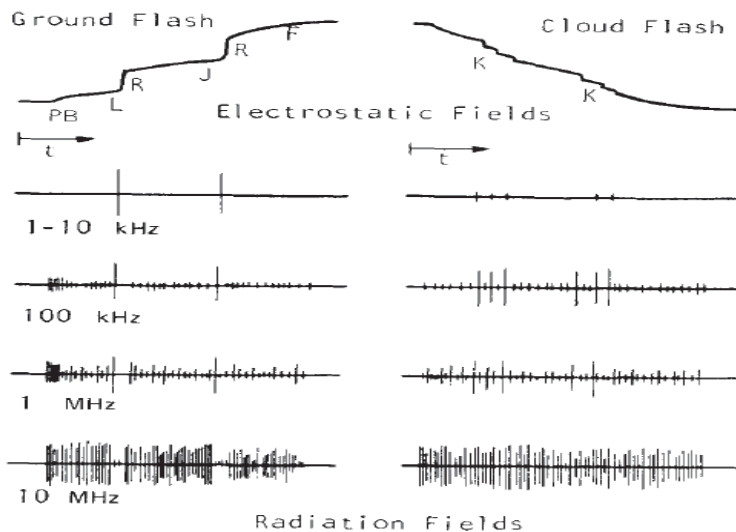

Fig. 4. Electromagnetic fields in lightning associated different channels, Preliminary Breakdown (PB), Leader (L), Return Stroke (R), Changes in (J, F and K). Adapted from ((Le Vine 1987)).

The major advantage of RF detection of lightning over optical is that optical detection is unable to distinguish many signatures like CG versus IC, RS, Leader and TIPPs etc. Also, the atmosphere has least effect on electromagnetic waves (Suszcynsky, Kirkland et al. 2000).

5. LiNSAT constellation, space and ground segments

5.1 Space segment
Space segment consists of constellation of three identical nano-satellites and each satellite is comprised of following units
- Attitude control through gravity gradient boom (GGB) Figure 5.
- Three orthogonal lightning antennas (GGB-LA, LA2, LA3), one antenna (GGB-LA) is integrated into GGB at nadir direction, Figure 5.
- Power subsystem (Solar panels, battery charge and discharge regulator (BCDR) and battery).
- Thermal subsystem
- VHF electronics
- Data processing unit (DPU)
- On-board event detector together with Adaptive Filtering
- Housekeeping
- Communication UHF/VHF monopole antenna (U-MP/V-MP): 2m and 70 cm frequency bands and S-band patch antenna

All subsystems are shown in Figure 6. The components selection criteria for on-board memory, telemetry volume, and power budget are the "cost effectiveness" therefore, commercial off the shelf components (COTS) will be used.

As a heritage from TUGSat1, the same Generic Nano-satellite Bus (GNB) (de Carufel 2009) will be used on LiNSAT with data rate from 32 – 256 kbps. Data volume per day will be ~ 15 MB/day. For LiNSAT, the actual amount of data is mode-dependent. The requirement of on-board memory with optimum data volume ~ 150 MB/day (3 GS) with 256 kbps data rate is possible. Based on studies done by the SPOT team (Barillot and Calvel 2002), around 8 events upset per year occur in LEO 800 km orbit. Countermeasures for the memory are necessary and the cold redundancy is considered. Additionally, a current limiter is foreseen to reset the experiment and the sub-systems on-board LiNSAT.

5.2 Constellation: local and global coverage
After launch and commissioning phase, all three satellites will be close together (local small scale coverage) and would be used for combined investigations (TOA). Due to natural orbital variations they separate from each other and, in the long run, the satellites will no longer remain in the constellation (global intermediate and large coverage). At this point they will be treated as individual entity (LiNSAT).

5.3 Ground segment
The global coverage emphasizes on the main purpose of ground segment as distributed GSs network (DGSN) to track the satellite and receive housekeeping and scientific data on global scale in real-time. DGSN consists of three GS
- Automated remote GS at Graz University of Technology, Austria (AR-TUG), (Jaffer and Koudelka 2011e)
- I-2-O gateway (Hermes-A) in Ecuador
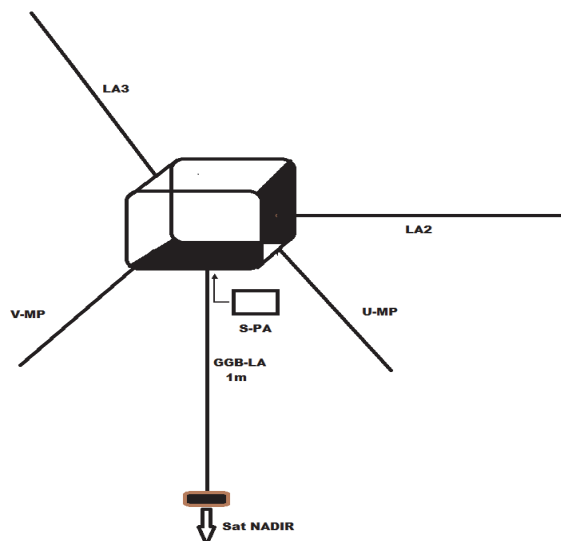- One proposed GS at Lahore, Pakistan (LiNSAT-GS)

Fig. 5. LiNSAT structure with antenna configuration of three orthogonal lightning antennas (GGB-LA, LA2 and LA3). GGB is a passive attitude control sub-system to nadir direction. Additionally the multi-purpose boom is integrated as lightning antenna.
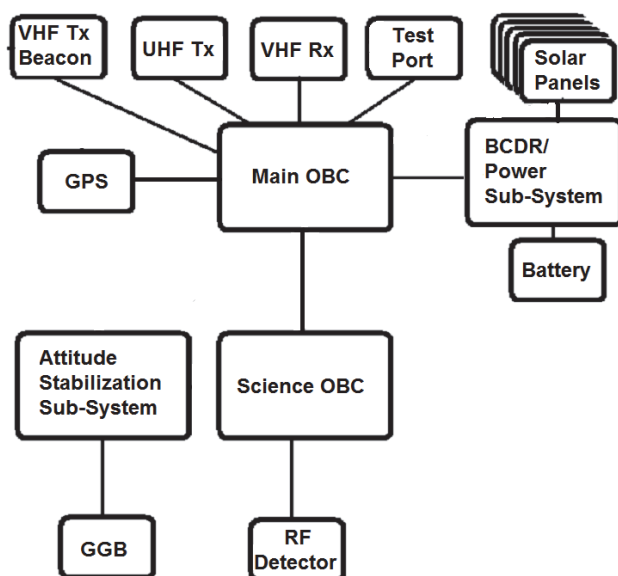
Fig. 6. Block diagram of all subsystems of LiNSAT. The science on-board computer (OBC) and ADCS OBC are connected to main OBC. Other subsystems like Communication and power are interfaced with main OBC.

First two GS are already functional and the third is proposed and we will pursue its development in near future.

From the scientific data reception point of view, DGSN opens up the mission to a wider range. Therefore, DGSN would eventually make difference as compared by the amount of data collected manually with standalone GS. Moreover, transformation of DGSN as autonomously operating network is foreseen. This would ultimately support future nano-satellite experiments effectively. Additionally, its scheduling capability which we pursue in near future will enhance its functionalities. The I-2-O gateway and virtual GS are detailed in (Jaffer, Klesh et al. 2010a; Nader, Carrion et al. 2010a; Jaffer, Nader et al. 2010b; Nader, Salazar et al. 2010b; Jaffer, Nader et al. 2010f; Jaffer, Nader et al. 2011a; Jaffer, Nader et al. 2011h; Jaffer, Nader et al. 2011i).The setup is shown in Figure 7.
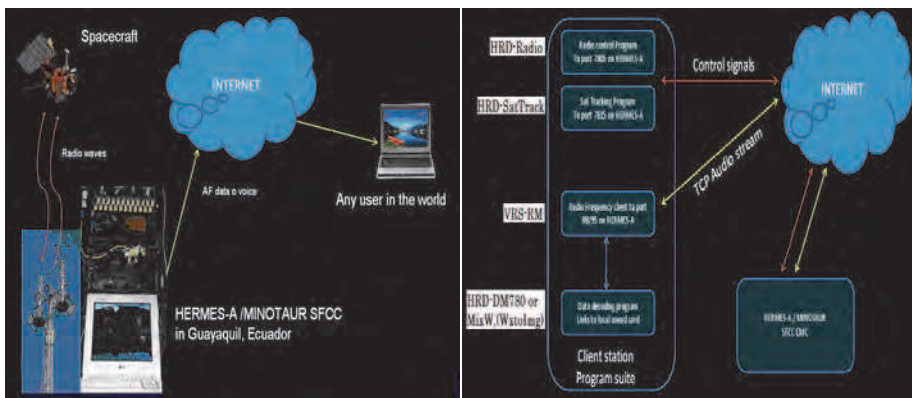

Fig. 7. LiNSAT ground segment, *Left*: HERMES-A set-up and working scenario, *Right*: virtual ground station at remote user end

5.4 LiNSAT modes of operation

LiNSAT consists of several mission modes (MO) of operation after successful deployment (Table 1). The LiNSAT is planned to perform functions in various modes depending upon task/ idle situations.

Mission Operation Mode No.	Tasks, Annotation
1	Deployment, *Commissioning phase*
2	Stabilization, *Commissioning phase*
3	Lightning Experiment, *Scientific Payload*
4	Ground Communication, *Telemetry*
5	Conserve Power/ Recharge, *in Eclipse*
6	Standby

Table 1. LiNSAT mission operational (MO) modes.

Modes 1 and 2 apply to initial deployment and stabilization of LiNSAT. Mode 3 is the key mode with five experiment mode options (Table 2). Switching to mode 4 occurs for telemetry operations. Mode 5 is applicable when the power subsystem is no longer capable to support normal operations, e.g. during eclipse. Mode 6 is the default mode when no other operations are going on. Either telemetry or lightning experiment will be carried out at a time for efficient use of on-board power.

For LiNSAT, EMC is a vital part to avoid intra- and inter-system disturbances from electromagnetic radiations and coupling with special considerations in the 20 - 40 MHz VHF range. The printed circuit board (PCB) layout tools considering routing and grounding concepts of the highly integrated electronics together with shielding and harness strategies. Verification on board level occurs with the aid of EMC pre-compliance measurements and validation of the system in an anechoic chamber. Fine tuning of the components and adaptive filtering (AF) of unwanted signals results in a high signal to noise ratio (SNR).

Electromagnetic pulses from DC converters could produce spurious signals similar to lightning spikes even in the same frequency range. Laboratory tests are currently carried out in order to optimize antenna, receiver and adaptive filter design.

The scientific payload on-board LiNSAT will perform detection of lightning events, measurement of time series and transmit to one of the GS within communication window. This mode is further sub-categorized and elaborated in (Table 2).

Experiment Mode	Tasks, Annotation
Survey Mode	Statistical; Number of lightning events above threshold level (coarse trigger)
Event Mode	Sferics time series data dumped into on-board memory
Background / CW Mode	All events/ signals, galactic, interference detected from ionosphere between two lightning events
Test Mode	Software test/ Polar lightning (If any)
EMC Mode	Artifacts from satellite itself

Table 2. LiNSAT experiment modes closely associated with mission modes (Table 1)

5.5 Payload instrumentation
5.5.1 Antennas and gravity gradient boom
The voltage received at LiNSAT

$$V = h_{eff}*E, \tag{1}$$

and depends on the lightning electrical field E and the effective length h_{eff} of the antenna. Also, $h_{eff} \sim h_m/2$ for $h_m \ll \lambda$, where h_m is the mechanical length of the antenna and λ the wavelength.

No stringent pointing requirements for LiNSAT are foreseen as compared with TUGSAT-1/BRITE, so a simple and inexpensive gravity gradient stabilization (GGS) technique already proven on many missions (NASA 2011b) and detailed in (Wertz and Larson 1999); (Wertz 1978) which points to the nadir of the satellites envisaged for satellite attitude control. The GGB fulfills the requirements and is selected due to its economical features like least power consumption (once during deployment) and the cheapest of all other stabilization mechanisms of the same breed.

The GGB, acting as an antenna for lightning detection, is a deployable with 10 % of the satellite mass (tip mass). A three-antenna system has multifold advantages, like redundant directional capability and simultaneous back up. In-orbit characteristics depend on several factors, e.g. mechanical forces, non-conservative forces and induced pendulum motions. The boom torque needs to overcome environmental torque for a maximized stabilization capability. The antenna works in non-resonant mode so lightning investigation is performed in different frequency ranges but with reduced efficiency.

5.5.2 Data Processing Unit (DPU)

The signal from the antenna is fed to the data processing unit (DPU) through a pre-amplifier prior to analog/digital conversion and further processing. As mentioned earlier, typical lightning electric fields at 1000 km altitude are 1mV/m at 40 MHz, 1 MHz bandwidth (Jacobson, Knox et al. 1999). After filtering and amplification, the 200 MS/s ADC will sample the received signals and the digitized signals are dumped into cyclic memory with the help of two levels of event detection (coarse and fine). Data acquisition captures a waveform record. A triggering unit helps in elimination of unwanted signals stemming from galactic and magnetospheric origins.

5.5.3 Data acquisition system (DAQ)

The data acquisition system (DAQ) is capable of retriggering a new record within microseconds of the end of the previous record. Data of many lightning events will be stored in cyclic memory/ buffer. The memory is capable to be overwritten all the times. A significant number of events can be stored in a solid-state mass memory before downloading via telemetry to the ground segment. The minimum telemetry transfer rate for science data is 180 kbytes per day. 256 MB of flash memory for long-term storage of measurement data are foreseen. The Sferics data will be identified with minimum pulse width ~ 50 μs and sharp rising amplitude with pulse rise time ~ 10 ns. The records will then be analyzed on ground to investigate VHF signatures in time and frequency domains. The payload configuration is shown in Figure 8.
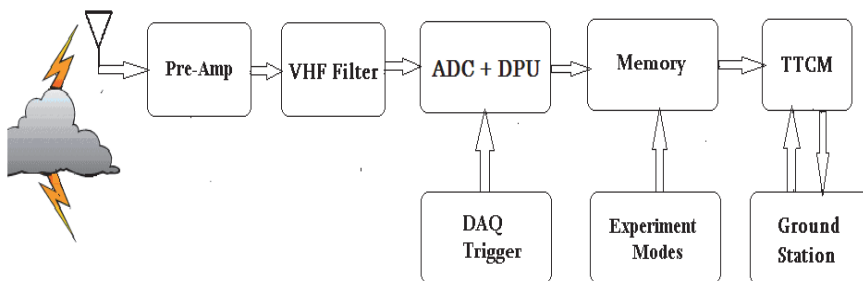

Fig. 8. Block diagram of LiNSAT scientific payload.

Event detector is an important part of the detection system; a signal processing subsystem performing various signal processing functions to classify the signals into distinct categories.

6. Adaptive filtering

The adaptive filtering (AF) structure shown in Figure 9 is based on and draws heritage from adaptive noise cancellation (ANC) (Haykin 1996). The input signal $d[k]$ is a lightning transient pulse that is contaminated with artifacts $a_d[k]$ from LiNSAT. The co-efficients for the reference signal $x[k]$ can be derived from two sources, either by ground-based EMC investigations as a preliminary estimation as pre-selector co-efficients for AF (GPC) or the output from the sensors on-board nano-satellite. The goal is to detect natural lightning spikes, so finally we'll have to rely on on-board sensor as an ultimate for updating the co-efficients of AF. The reason behind could be

- slightly shifting of subsystems emissions curve within scientific payload measurement range
- cancellation of disturbances generated by LiNSAT or subsystems, $a_x[k]$.

Electric field emissions in the measurement range 20-40 MHz, from on-board subsystems has got an emission curve as a proxy of the artifacts generated by LiNSAT. Being a narrowband disturbance, it will be eliminated using a notch filter. It can happen that the frequency of the emission curve shifts within the measurement range, therefore, we need to update the filter co-efficients to track the movement in a robust manner.

We are using coarse and fine triggering mechanism for the lightning detector on-board LiNSAT and the adaptive filtering approach will be used in coincidence with the fine trigger on-board the satellite (DAQ Trigger, Figure 8) for redundancy.

The orbital footprint of the LiNSAT will be scanning the whole Earth during several orbits but as we know the lightning flash rate varies along the orbit from the poles to equator as shown in Figure 2. This is valuable statistical environmental input for the $d[k]$ channel for precise triggering and to avoid false alarms.
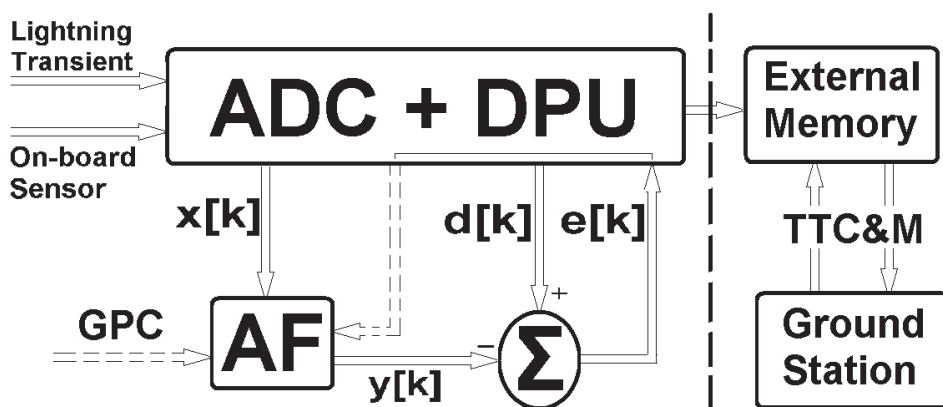

Fig. 9. DAQ trigger for lightning detector on-board LiNSAT based on adaptive filters

$x[k]$ is a digitized output of the sensor on-board which detects artifacts in terms of electric field emissions for LiNSAT itself. This could be broadband or narrowband, e.g. a clock signal or harmonics of the digital electronics

$$x[k] = a_x[k]. \tag{2}$$

$d[k]$ is digitized signal of the lightning transient after passing through antenna, VHF filter and pre-amplification including noise picked up in this receiving channel,

$$d[k] = s[k] + a_d[k], \tag{3}$$

where $a_d[k]$ and $a_x[k]$ are correlated noise sources.

AF is an FIR filter while the initial co-efficients for the filter are derived from ground based investigations (GPC) during development phase.

$y[k]$ is the output of the AF that sums up with $d[k]$ to produce error signal that ultimately is used for

1. Trigger purpose for the on-board lightning detector to dump the ring buffer/ cyclic memory contents into external memory for future download using telemetry, tracking, command and monitoring (TTC&M) by one of the ground stations through visibility/ communication window
2. To modify the coefficients of the AF accordingly using LMS algorithm.

Among several requirements, e.g. robustness, tracking speed and stability of the AF, the on-board computational power of the DPU is one of the constraints in space.

The filter is in the digital domain and is application dependent. The output is noise-removed lightning signal which will trigger the ring buffer to store the transients for future download through all three GS.

To determine the capability of the filter, we tested it with real life signals i.e. artificial discharges in high voltage chamber (section 9.2) and natural signals (section 9.3) in particular TIPP event recorded by ALEXIS satellite (Massey, Holden et al. 1998; Jacobson, Knox et al. 1999). The outputs were found to be as close as noise-free real lightning transients. The major advantage of the output (error signal) is that it would trigger the memory (on-board LiNSAT) with lower threshold level. Therefore, lightning pulses with even small peaks will be captured using adaptive filter fine trigger, otherwise would be hard to capture due to higher noise floor. The out puts are shown in Figure 10 and Figure 11.

The code to generate through such signals using AF through Matlab function is elaborated in Table 3.

```
function
[E,Y,noise,sig_plus_filterednoise]=anc_lightning(signal,filterorder,cutoff_frequency)
% [E,Y,noise,sig_plus_filterednoise]=anc_lightning(b23(1.18*10^6:1.28*10^6,1),4,0.4);
noise=0.1*randn(length(signal),1); …………………% noise modeling
nfilt=fir1(filterorder,cutoff_frequency)'; ……………% filter order LP
fnoise=filter(nfilt,1,noise); ……………………………% correlated noise data
sig_plus_filterednoise=signal+fnoise; ………….....% input plus noise
coeffs=nfilt-0.01; ………………………………………% filter initial conditions
mu=0.05; …………………………………………………% step size for algorithm updating
S=initlms(coeffs,mu); …………………………………% Init LMS FIR filter
[Y,E,S]=adaptlms(noise,sig_plus_filterednoise,S);...% Y=filtered data, E=Prediction Error
```
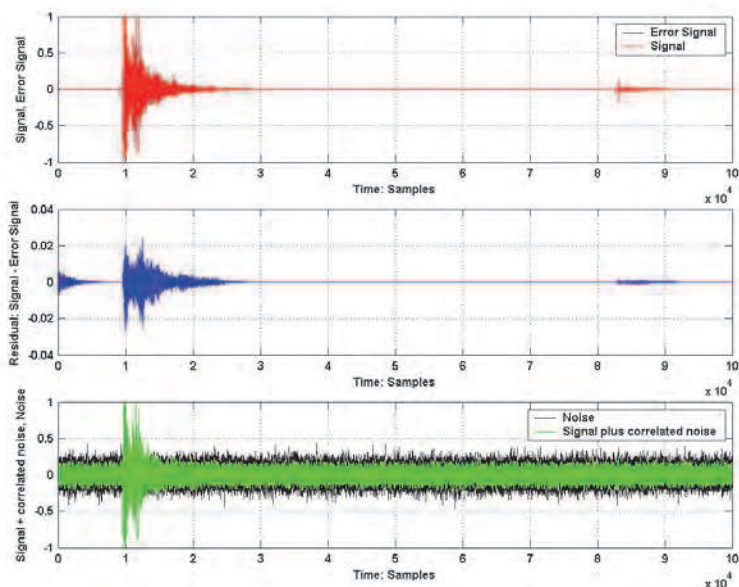
Table 3. Matlab code to test Adaptive filter algorithm

Fig. 10. Acoustic signal generated in high voltage chamber and received using Adaptive filter.

The other signal of interst to test AF is natural lightning (i.e. TIPP) captured with ALEXIS satellite shown in Figure 11. Again, the noise-removed signal can be observed.
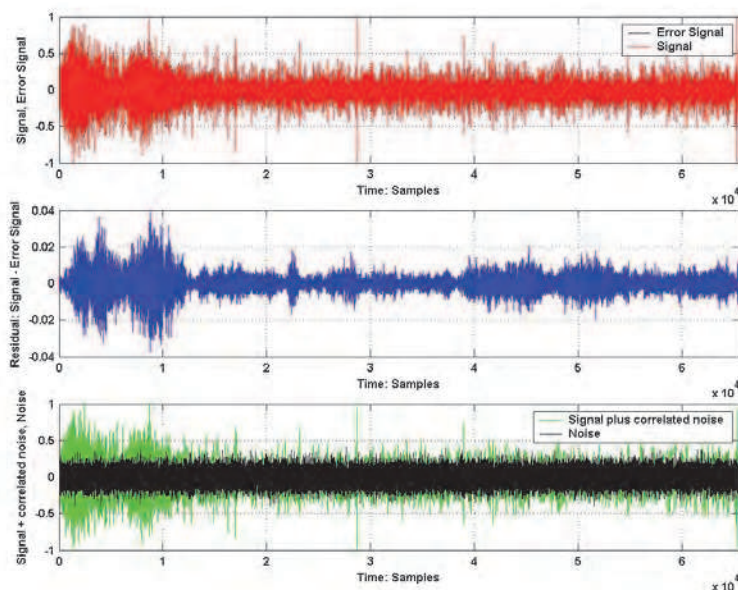

Fig. 11. TIPP event captured with Adaptive filter. The error signal is close to real input, an advantage of using AF to trigger on-board memory for saving noise-free transients.

Based on previous experiments using engineering models and TUGSat-1 study, the DAQ power estimations are ~ 3 W on average up to 5 W (peaks) for short time. Power consumption is mainly determined by the consumption of digital electronics. Among several requirements, e.g. robustness, tracking speed and stability of the AF, the on-board computational power of the DPU is one of the constraints in space. A technique to overcome this deficiency on-board is power aware computing (Graybill and Melhem 2002) and one case-study for FORTE mission is discussed in (Shriver, Gokhale et al. 2002).

7. Attitude control system

Unlike TUGSat-1/ BRITE-Austria which is three-axis stabilized, LiNSAT will use the widely used and inexpensive gravity gradient stabilization (GGS) technique for its attitude control. The deployable GGB has a length of 1 m. The vector of the boom and its counterweight will be rotating around a vector pointing directly towards the center of the Earth. If this oscillation can be dampened, it is possible to control the attitude of the satellite such that the nadir surface points towards the Earth within limits of $\pm 10°$, (Taylor-University 2011). This is sufficient for antenna pointing. The setup from Figure 5 benefits from the RF noise survey (Burr, Jacobson et al. 2004; Burr, Jacobson et al. 2005) and enables investigations of major types of lightning, including TIPPs (Holden, Munson et al. 1995; Massey and Holden 1995; Massey, Holden et al. 1998; Tierney, Jacobson et al. 2002).

A redundant approach (passive magnetic and GGB) is being used by Quakesat (Quakesat 2011). It used GGB back in 2003 and still operating. The ADCS of this satellite is primarily a magnet, but it extends a magnetotorquer out on a boom providing more than the average effects from gravitational gradient. As without a large tip mass, the gravity gradient effect is reduced, so magnets are needed to reduce damping effects and ultimately stabilizing pointing accuracy.

The tip mass is comparable to total mass of the satellite (10%). In principle the GGB works for imaging payload with a pointing accuracy ~ ± 5, but roll of the satellite must be taken into account. There are only a few small satellites with "camera" as optical payload using GGB and/ or passive magnets (no 3-axis ADCS) and manage the pointing requirements. Although for communication link, GGB technique works well as long as we assume the roll rate is slow, we can probably take a picture without smear, but only if the assumption holds or the camera is designed to counterbalance this rolling effect.

8. Experimental setup and results

8.1 Lightning detection simulation

In Austria, lightning flash density is between 0.5 and 4 flashes per square km per year, depending on terrain (Diendorfer, Schulz et al. ; Schulz and Diendorfer 1999; Diendorfer, Schulz et al. 2002; Schulz and Diendorfer 2004; Schulz, Cummins et al. 2005). Lightning flash occurrence duration is about half a second. The simulated signals are evaluated with coarse and fine triggered detection using "lightning detector" program written in Matlab. Also, execution and processing time of 10,000 data points are checked in Matlab on standard PC and will be compared to Microprocessor time after transformation into machine language. Execution time in Matlab found to be 5 s on the average. As the algorithm contains many loops, so the computation time is higher.

The blocks of the receiving chain (Figure 8) are simulated individually and as a whole using Matlab functions. To verify the simulations, lab measurements (RF and Acoustic) are performed. The objective of these measurements/ simulations was to find algorithm which could implemented on the on-board lightning detector electronics (requirements: must be fast, effective and running with limited resources).

One second lightning strokes data for simulation using the program is analyzed. The program computes the pulse width, pulse rise time, number of detected pulses, frequency and pulse-amplitude and stores all the information in a resultant matrix; emulation of cyclic memory. The algorithm is mode dependent and basically captures lightning signals above threshold level. It classifies and characterizes the pulses. A standard class of lightning signals was used to see e.g. total electron contents (TEC) effects on lightning transients passing through ionosphere. The algorithm will work along with experiment modes (Table 2).

For coarse detection, the whole window was divided in one thousand 1 ms sub-windows for computing mean and standard deviation (power) in each sub-window above threshold level of noise floor. This procedure will help us in pre-selection of the data and to change the experimental modes. Telemetry using coarse trigger will be downloaded for ground based analysis. The resultant matrix of the program is shown in Figure 12. Other consideration is mode-switching while above Equator, Poles etc with the lightning detector on-board LiNSAT.

```
    PULSE=>No.   Start-Time  Widthth  thLevel  AmplitudeRMS  Rise-Time  Max-Frequency

resultantMatrix =

       1.0000      4.0000    2.0000   16.0000    17.3449      17.8759      0.0196
       2.0000      7.0000    2.0000   16.0000    17.9203      21.3362      0.0164
       3.0000     13.0000    2.0000   16.0000    19.1966      28.3573      0.0123
       4.0000     19.0000    3.0000   16.0000    18.0037      33.4029      0.0105
       5.0000     27.0000    1.0000   16.0000    17.6707      41.1366      0.0085
       6.0000     31.0000    1.0000   16.0000    22.0093      48.6074      0.0072
       7.0000     34.0000    1.0000   16.0000    21.3789      51.1032      0.0068
       8.0000     37.0000    2.0000   16.0000    21.6722      54.3378      0.0064
       9.0000     40.0000    1.0000   16.0000    16.7201      53.3761      0.0066
      10.0000     47.0000    1.0000   16.0000    22.8012      65.2410      0.0054
      11.0000     50.0000   12.0000   16.0000   134.4105     157.5284      0.0022
      12.0000     64.0000    2.0000   16.0000    19.4476      79.5581      0.0044
      13.0000     70.0000    1.0000   16.0000    21.2800      87.0240      0.0040
      14.0000     74.0000    2.0000   16.0000    18.5694      88.8555      0.0039
      15.0000     78.0000    2.0000   16.0000    17.2528      91.8023      0.0038
      16.0000     81.0000    1.0000   16.0000    19.4400      96.5520      0.0036
      17.0000     84.0000    1.0000   16.0000    21.9625     101.5700      0.0034
      18.0000     88.0000    1.0000   16.0000    20.0368     104.0295      0.0034
      19.0000     92.0000    1.0000   16.0000    21.6809     109.3447      0.0032
      20.0000     98.0000    1.0000   16.0000    18.6548     112.9238      0.0031
```

Fig. 12. Matlab™ simulated results of the program "lightning detector". In this computation, threshold level for coarse detection is set to 16 mV to extract all pulses above noise floor. Twenty pulses were detected along with their information about pulse start time, pulse rise/ fall time, amplitude and maximum frequency.

8.2 Artificial lightning measurement campaigns
8.2.1 Electrical discharges in high voltage chamber

In these measurement campaigns, artificial lightning was produced in laboratory at Space Research Institute, Austrian Academy of Sciences, Graz and Institute of High voltage Technology and System Management of the Graz University of Technology high voltage chamber. The artificial lightning discharge was from 700 kV to ~ 1.8 MV under normal pressure and temperature conditions. The system has selectable +ve and –ve polarity and electrodes inter-distance. Two discharges using different models are shown in Figure 13. The lightning measurement setup consisted of electric field probe (60 Hz to 100 MHz) and digital oscilloscope (bandwidth = 200 MHz) with external and manual trigger (pre-, post-trigger) option.

We focus mainly on the received time series including noisy features to extract characteristic parameters. We determined the chamber inter-walls distance by considering reflections in the measurement. Round-trip-time (direct and reflected) waves indicate many reflections from all walls of the chamber. The captured image shows similarities with natural lightning signal shown in Figure 20. All experimental evidences are shown in figures below.

Fig. 13. *Left*: Lightning event occurrence on a model. Also branched lightning (to ground and air) was observed. *Right:* Color changes (intensity) due to discharges along the rope. The variations indicate current interaction with fibers of the rope under impact of lightning discharge of ~ 1.8 MV. Post-event inspection revealed no damage in the rope, macroscopically.
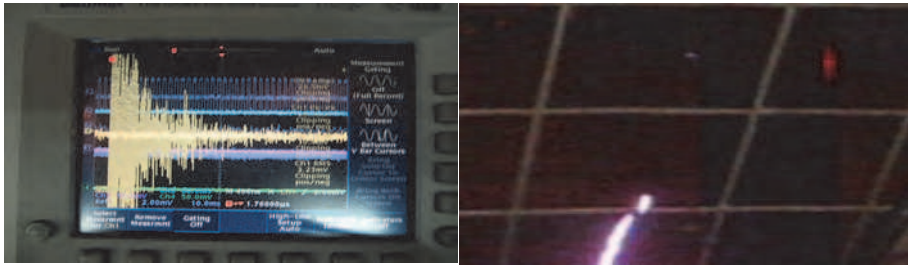
Fig. 14. *Left*: Lightning electric field captured with oscilloscope. A round-trip-time (direct and reflected) wave indicates many reflections from all walls of the chamber. The captured image shows similarities with natural lightning signal shown in Figure 20, *Right*: The striking phenomenon, upward lightning initiated by sharp objects in the vicinity of chamber ground was observed. In principle, this phenomenon occurs with sharp endings tall buildings like church etc. It has similarity with return stroke (RS) phenomenon.

Fig. 15. *Left*: Basic structure of the tent as a model for the Faraday cage. There can be arcing if some metal is present inside the tent (no lightning safety), *Mid*: Lightning event occurs near the object due to slight moment of the electrode. *Right*: The measured electric field due to arcing (impact) of the lightning discharge on the model of Faraday cage.

8.2.2 Acoustic measurement

We performed acoustic measurements in parallel to RF detection of artificial lightning in high voltage chamber (Eichelberger, Prattes et al. 2010; Eichelberger, Prattes et al. 2011). The outcomes helped to correlate RF signatures.

8.2.3 Electrical discharges in a lab

Besides the measurements from the previous section, we wanted to determine all associated phenomena with natural lightning, e.g. corona discharges, glow and sparks. Moreover, these phenomena were easily produced in the lab due to controlled setup. But it was not necessary to perform these measurements in the high voltage chamber. This setup helps to investigate distinct features of all three mentioned discharge types and the transition among all these phenomena related to voltage in a pre-defined setup.

The setup comprises of

- High voltage power supply unit (HV-PSU)
- Adjustable electrodes: a metal plate (Anode) and screw (Cathode) combination with inter-distance of ~ 1 inch (2.54 cm)
- Electric field probe (60 Hz to 100 MHz)
- Digital Oscilloscope (eTek, 200 MHz bandwidth)

8.2.3.1 Corona discharges

The very first broadband phenomenon occurs with a hissy sound due to increase in the voltage. The maximum corona acoustic along with glow was observed at 11 – 12 kV.
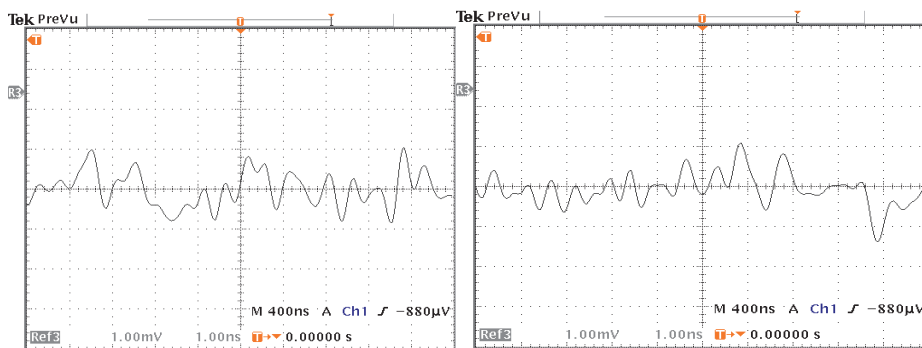

Fig. 16. eTek Oscilloscope display of Corona discharges.

8.2.3.2 Glow discharges
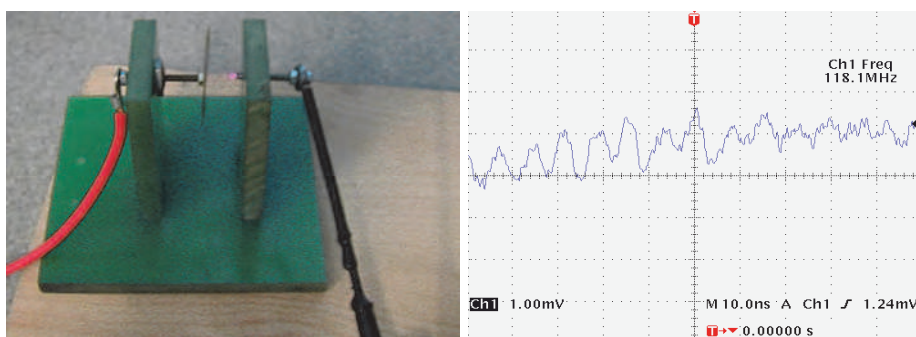
Fig. 17. *Left*: Artificial lightning: indication of corona and glow discharge, *Right*: Glow discharge measurement. Frequency ~ 118 MHz. Applied Voltage is 11 kV. The maximum corona sound with glow was observed at 11 - 12 kV and decaying afterwards.

8.2.3.3 Spark discharges

The HF and VHF radiations associated with initial breakdown pulse in cloud flashes were studied by (Krider, Weidman et al. 1979) and they found that radiations at 3 MHz, 69 MHz, 139 MHz and 259 MHz tend to peak during the initial half cycle of the pulse. We have also observed the feature in the lab at 139.6 MHz shown in Figure 18.
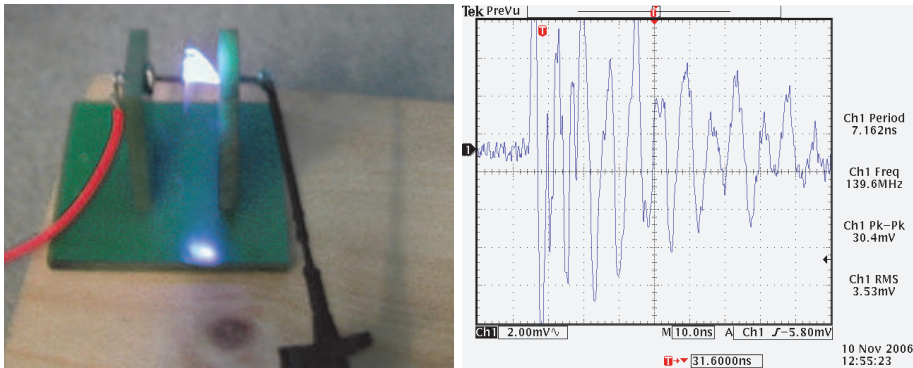
Fig. 18. *Left*: Artificial lightning, spark discharges on cathode. The maximum frequency observed for spark was 140 MHz. The spark was produced at 13 kV and higher voltages, *Right*: Spark discharge measurement, the maximum frequency observed for Spark is 140 MHz. The spark produced at 13 kV and higher, also measured on oscilloscope.

8.3 Natural lightning measurement

During intense thunderstorm activity on June 30, 2010, in urban area of Graz, Austria, natural lightning measurements were performed using broadband discone antenna, 15 m shielded cable and digital oscilloscope (Bandwidth = 200 MHz) to correlate with artificial lightning discharges measured in high voltage chamber. The radiation patterns of such antenna are shown in Figure 19.
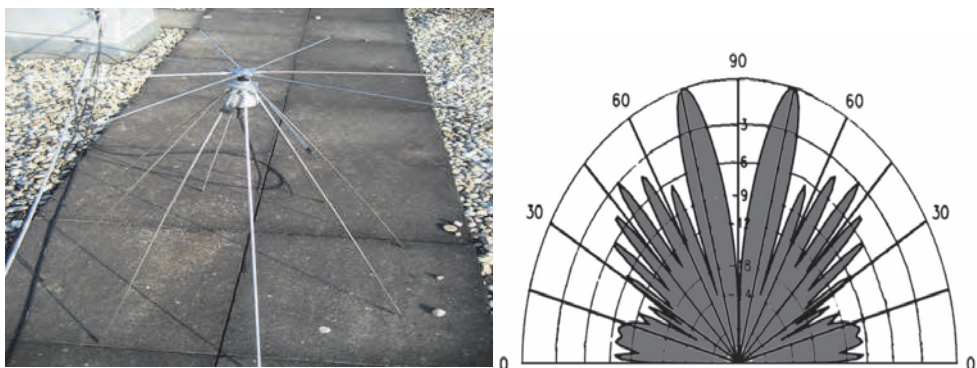

Fig. 19. *Left*: The broadband discone antenna used for natural lightning measurements. The antenna was put on roof of the Graz University of Technology building for better reception and to avoid interferences within the campus, *Right*: Radiation patterns of discone antenna (DA-RP 2011).
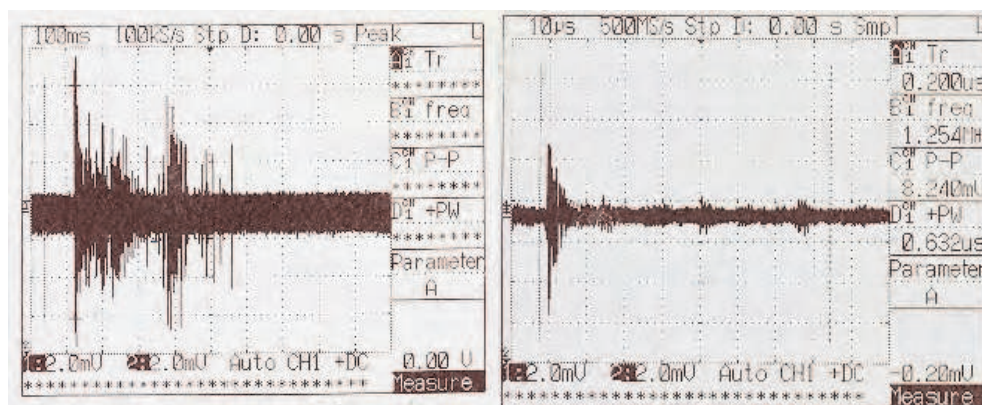
Fig. 20. *Left*: Natural lightning measurement with digital oscilloscope (Bandwidth = 200 MHz), with sampling rate 100 kS/s. It shows two individual strokes within a lightning flash, *Right*: Natural lightning measurement with digital oscilloscope (Bandwidth = 200 MHz) with sampling rate 500 MS/s indicates a single stroke with a few reflections.

No.	$f_{sampling}$	V_{p-p}	V_{noise}	t_{rise}	t_{fall}	$t_{inter-pulse}$
Figure 20 (Left)	100 kS/s	18 mV	2 mV	10 ms	200 ms	250 ms
Figure 20(Right)	500 MS/s	6 mV	1 mV	1 μs	5 μs	15 μs

$f_{sampling}$	Sampling frequency of the oscilloscope
V_{p-p}	Peak-to-peak voltage
V_{noise}	Noise floor
t_{rise}	Pulse rise time (10-90% of the peak voltage)
t_{fall}	Pulse fall time (90-10% of the peak voltage)
$t_{inter-pulse}$	Time between two pulses (reflections, TIPP etc)

Table 4. Natural lightning: setup and obtained resultant parameters

9. Data analysis conclusions

The measurements from the HV chamber and natural environment have been evaluated in the time domain. We also determined statistically that how the rise/ fall time for each stroke is different and relevant to indicate unique signature of each sub-process of lightning event. The envelope of the signal is analyzed

- Events: by coinciding the size of the HV chamber (reflections) with the signal trace
- The ambient noise (and carrier) properties in these measurements
- Out of these results we have deduced the requirements for the lightning electronics of the LiNSAT (sample rate, buffer size, telemetry rate)
- The Fourier transform of the signals (frequency domain) helped in indicating the bandwidth of the lightning detector on-board LiNSAT.

10. Summary and conclusions

We presented a feasibility study of LiNSAT for lightning detection and characterization as part of climate research with low-cost scientific mission, carried out in the frame of university-class nano-satellite mission. In order to overcome the mass, volume and power constraints of the nano-satellite, it is planned to use the gravity gradient boom as a receiving antenna for lightning Sferics and to enhance the satellite's directional capability.

We described an architecture of a lightning detector on-board LiNSAT in LEO. The LiNSAT will be a follow-up mission of TUGSat1/BRITE and use the same generic bus and mechanical structure. As the scientific payload is lightning detector and it has no stringent requirement of ADCS to be three axis stabilization, so GGS technique is more suitable for this mission.

In this chapter we elaborated results of two measurement campaigns; one for artificial lightning produced in high voltage chamber and lab, and the second for natural lightning recorded at urban environment. We focused mainly on the received time series including noisy features and narrowband carriers to extract characteristic parameters. We determined the chamber inter-walls distance by considering reflections in the first measurements to correlate with special lightning event (TIPPs) detected by ALEXIS satellite.

The algorithm for the instruments on-board electronics has been developed and verified in Matlab™. The time and frequency domain analysis helped in deducing all the required parameters of the scientific payload on-board LiNSAT.

To avoid false signals detection (false alarm), pre-selectors on-board LiNSAT are part of the Sferics detector. Adaptive filters are formulated and tested with Matlab functions using artificial and real signals as inputs. The filters will be developed to differentiate terrestrial electromagnetic impulsive signals from ionospheric or magnetospheric signals on-board LiNSAT.

11. Acknowledgements

12. References

Barillot, C. and P. Calvel (2002). "Review of commercial spacecraft anomalies and single-event-effect occurrences." Nuclear Science, IEEE Transactions on 43(2): 453-460.

Burr, T., A. Jacobson, et al. (2004). "A global radio frequency noise survey as observed by the FORTE satellite at 800 km altitude." Radio Science 39(4).

Burr, T., A. Jacobson, et al. (2005). "A dynamic global radio frequency noise survey as observed by the FORTE satellite at 800 km altitude." Radio Science 40(6).

DA-RP (2011). http://www.moonraker.com.au/techni/discs&cones.htm.

de Carufel, G. (2009). Assembly, Integration and Thermal Testing of the Generic Nanosatellite Bus, University of Toronto.

Diendorfer, G., W. Schulz, et al. Comparison of correlated data from the Austrian lightning location system and measured lightning currents at the Peissenberg tower.

Diendorfer, G., W. Schulz, et al. (2002). "Lightning characteristics based on data from the Austrian lightning locating system." Electromagnetic Compatibility, IEEE Transactions on 40(4): 452-464.

Eichelberger, H., G. Prattes, et al. (2010). Acoustic measurements of atmospheric electrical discharges for planetary probes. European Geosciences Union (EGU). Vienna, Austria.

Eichelberger, H., G. Prattes, et al. (2011). Acoustic outdoor measurements with a multi-microphone instrument for planetary atmospheres and surface. European Geosciences Union (EGU). Vienna, Austria.

Fulchignoni, M., F. Ferri, et al. (2005). "In situ measurements of the physical characteristics of Titan's environment." Nature 438(7069): 785-791.

Graybill, R. and R. Melhem (2002). Power aware computing, Plenum Pub Corp.

Haykin, S. (1996). Adaptive Filter Theory, Prentice Hall.

Holden, D., C. Munson, et al. (1995). "Satellite Observations of Transionospheric Pulse Pairs." Geophys. Res. Lett. 22(8): 889-892.

Jacobson, A., S. Knox, et al. (1999). "FORTE observations of lightning radio-frequency signatures: Capabilities and basic results." Radio Sci. 34(2): 337-354.

Jacobson, A. R., S. O. Knox, et al. (1999). "FORTE observations of lightning radio-frequency signatures: Capabilities and basic results." Radio Sci. 34(2): 337 - 354.

Jaffer, G. (2006b). Measurements of electromagnetic corona discharges. Educational workshop: "Lehrerfortbildung des Pädagogischen Institutes des Bundes in Steiermark: von Monden, Kometen und Planeten im Sonnensystem" Space Research Institute, Austrian Academy of Sciences , Graz, Austria.

Jaffer, G. (2011c). Austrian Lightning Nanosatellite (LiNSAT): Space and Ground Segments. 3rd International Conference on Advances in Satellite and Space Communications (SPACOMM 2011). Budapest, Hungary. (accepted).

Jaffer, G., H. U. Eichelberger, et al. (2010d). LiNSAT: Austrian lightning nano-satellite. UN-OOSA/Austria/ESA Symposium on Small Satellite Programmes for Sustainable Development: Payloads for Small Satellite Programmes. Graz, Austria.

Jaffer, G., A. Klesh, et al. (2010a). Using a virtual ground station as a tool for supporting higher education. 61st International Astronautical Congress (IAC). Prague, Czech Republic.

Jaffer, G. and O. Koudelka (2011d). Lightning detection onboard nano-satellite (LiNSAT). International Conference on Atmospheric Electricity (ICAE). Rio de Janeiro, Brazil. (accepted).

Jaffer, G. and O. Koudelka (2011e). Automated remote ground station for Austrian lightning nanosatellite (LiNSAT). 8th IAA Symposium on Small Satellites for Earth Observation. Berlin, Germany,, (accepted). (accepted).

Jaffer, G., O. Koudelka, et al. (2008). The detection of sferics by a nano-satellite. 59th International Astronautical Congress (IAC). Glasgow, UK 8.

Jaffer, G., O. Koudelka, et al. (2010e). A Lightning Detector Onboard Austrian Nanosatellite (LiNSAT). American Geophysical Union, Fall Meeting`.

Jaffer, G., R. Nader, et al. (2010b). Project Agora: Simultaneously downloading a satellite signal around the world. 61st International Astronautical Congress (IAC). Prague, Czech Republic: 8.

Jaffer, G., R. Nader, et al. (2011a). "Using a virtual ground station as a tool for supporting space research and scientific outreach." Acta Astronautica (in press).

Jaffer, G., R. Nader, et al. (2011h). Online and real-time space operations using Hermes-A I-2-O gateway. 1st IAA Conference On University Satellites Missions. Rome, Italy: -.

Jaffer, G., R. Nader, et al. (2011i). "Online and real-time space operations using Hermes-A I-2-O gateway." Actual Problems of Aviation and Aerospace Systems (submitted).

Jaffer, G., R. Nader, et al. (2010f). An online and real-time virtual ground station for small satellites, UN-OOSA/Austria/ESA Symposium on Small Satellite Programmes for Sustainable Development: Payloads for Small Satellite Programmes.

Jaffer, G. and K. Schwingenschuh (2006a). Lab experiments of corona discharges. Graz, Austria, Space Research Institute (IWF), Austrian Academy of Sciences. 37.

Koudelka, O., G. Egger, et al. (2009). "TUGSAT-1/BRITE-Austria-The first Austrian nanosatellite." Acta Astronautica 64(11-12): 1144-1149.

Krider, E., C. Weidman, et al. (1979). "The Temporal Structure of the HF and VHF Radiation Produced by Intracloud Lightning Discharges." J. Geophys. Res. 84(C9): 5760-5762.

Le Vine, D. M. (1987). "Review of measurements of the RF spectrum of radiation from lightning." Meteorology and Atmospheric Physics 37(3): 195-204.

Massey, R. and D. Holden (1995). "Phenomenology of transionospheric pulse pairs." Radio Sci. 30(5): 1645-1659.

Massey, R., D. Holden, et al. (1998). "Phenomenology of transionospheric pulse pairs: Further observations." Radio Sci. 33(6): 1755-1761.

Massey, R. S., D. N. Holden, et al. (1998). "Phenomenology of transionospheric pulse pairs: Further observations." Radio Science 33(6): 1755-1761.

Nader, R., H. Carrion, et al. (2010a). HERMES Delta: The use of the DELTA operation mode of the HERMESA/ MINOTAUR Internet-to-Orbit gateway to turn a laptop in to a virtual EO ground station. 61st International Astronautical Congress (IAC). Prague, Czech Republic

Nader, R., P. Salazar, et al. (2010b). The Ecuadorian Civilian Space Program: Near-future manned research missions in a low cost, entry level space program. 61st International Astronautical Congress (IAC). Prague, Czech Republic

NASA (2011a). http://thunder.msfc.nasa.gov/data/query/mission.png.

NASA (2011b). http://science.nasa.gov/missions/ats/.

Price, C. and D. Rind (1993). "What determines the cloud to ground lightning fraction in thunderstorms?" Geophysical Research Letters 20(6): 463-466.

Quakesat (2011). http://www.quakefinder.com/joomla15/index.php.

Rakov, V. A. and M. A. Uman (2003). Lightning: physics and effects, Cambridge Univ Pr.

Schulz, W., K. Cummins, et al. (2005). "Cloud-to-ground lightning in Austria: A 10-year study using data from a lightning location system." J. Geophys. Res. 110(D9): 1-20.

Schulz, W. and G. Diendorfer (1999). Lightning Characteristics as a function of altitude evaluated from lightning location network data, SOC AUTOMATIVE ENGINEERS INC.

Schulz, W. and G. Diendorfer (2004). Lightning peak currents measured on tall towers and measured with lightning location systems.

Schwingenschuh, K., B. P. Besser, et al. (2007). HUYGENS in-situ observations of Titan's atmospheric electricity. European Geosciences Union (EGU) General Assembly. Vienna, Austria.

Schwingenschuh, K., R. Hofe, et al. (2006a). In-situ observations of electric field fluctuations and impulsive events during the descent of the HUYGENS probe in the atmosphere of Titan. European Planetary Science Congress. Berlin, Germany. 37: 2793.

Schwingenschuh, K., R. Hofe, et al. (2006b). Electric field observations during the descent of the HUYGENS probe: evidence of lightning in the atmosphere of Titan. 36th COSPAR Scientific Assembly. Beijing, China. 37: 2793.

Schwingenschuh, K., H. Lichtenegger, et al. (2008b). Electric discharges in the lower atmosphere of Titan: HUYGENS acoustic and electric observations. 37th COSPAR Scientific Assembly. Montral, Canada. 37: 2793.

Schwingenschuh, K., G. J. Molina-Cuberos, et al. (2001). "Propagation of electromagnetic waves in the lower ionosphere of Titan." Io, Europa, Titan and Cratering of Icy Surfaces, Advances of Space Research 28(10): 1505-1510.

Schwingenschuh, K., T. Tokano, et al. (2010). Electric field transients observed by the HUYGENS probe in the atmosphere of Titan: Atmospheric electricity phenomena or artefacts? 7th International Workshop on Planetary, Solar and Heliospheric Radio Emissions (PRE VII) Graz, Austria

Shriver, P. M., M. B. Gokhale, et al. (2002). A power-aware, satellite-based parallel signal processing scheme, Power aware computing, Kluwer Academic Publishers, Norwell, MA.

Suszcynsky, D. M., M. W. Kirkland, et al. (2000). "FORTE observations of simultaneous VHF and optical emissions from lightning: Basic phenomenology." Journal of Geophysical Research-Atmospheres 105(D2): 2191-2201.

Taylor-University (2011). GGB Design Document.

Tierney, H. E., A. R. Jacobson, et al. (2002). "Transionospheric pulse pairs originating in maritime, continental, and coastal thunderstorms: Pulse energy ratios." Radio Sci. 37(3).

Uman, M. A. (2001). The lightning discharge, Dover Pubns.

Volland, H. (1995). Handbook of atmospheric electrodynamics, CRC.

Wertz, J. R. (1978). Spacecraft attitude determination and control, Kluwer Academic Pub.

Wertz, J. R. and W. J. Larson (1999). "Space mission analysis and design."

Williams, E. R., M. E. Weber, et al. (1989). "The Relationship between Lightning Type and Convective State of Thunderclouds." Journal of Geophysical Research-Atmospheres 94(D11): 13213-13220.

Adaptive Filtering Applications

Edited by Dr Lino Garcia

Adaptive filtering is useful in any application where the signals or the modeled system vary over time. The configuration of the system and, in particular, the position where the adaptive processor is placed generate different areas or application fields such as: prediction, system identification and modeling, equalization, cancellation of interference, etc. which are very important in many disciplines such as control systems, communications, signal processing, acoustics, voice, sound and image, etc. The book consists of noise and echo cancellation, medical applications, communications systems and others hardly joined by their heterogeneity. Each application is a case study with rigor that shows weakness/strength of the method used, assesses its suitability and suggests new forms and areas of use. The problems are becoming increasingly complex and applications must be adapted to solve them. The adaptive filters have proven to be useful in these environments of multiple input/output, variant-time behaviors, and long and complex transfer functions effectively, but fundamentally they still have to evolve. This book is a demonstration of this and a small illustration of everything that is to come.

How to reference

In order to correctly reference this scholarly work, feel free to copy and paste the following:

Ghulam Jaffer, Hans U. Eichelberger, Konrad Schwingenschuh and Otto Koudelka (2011). A LEO Nano-Satellite Mission for the Detection of Lightning VHF Sferics, Adaptive Filtering Applications, Dr Lino Garcia (Ed.), ISBN: 978-953-307-306-4, InTech, Available from: http://www.intechopen.com/books/adaptive-filtering-applications/a-leo-nano-satellite-mission-for-the-detection-of-lightning-vhf-sferics

INTECH
open science | open minds